.20

Data-Driven Adaptive Second-Order Sliding Mode Control with Noisy Data ⋆

Behrad Samari [a], Gian Paolo Incremona [b], Antonella Ferrara [c], Abolfazl Lavaei [a]

[a] *School of Computing, Newcastle University, United Kingdom*

[b] *Dipartimento di Elettronica, Informazione e Bioingegneria, Politecnico di Milano, Italy*

[c] *Dipartimento di Ingegneria Industriale e dell'Informazione, University of Pavia, Italy*

Abstract

This paper offers a data-driven approach for designing adaptive suboptimal second-order sliding mode (ASSOSM) controllers for single-input nonlinear systems, characterized by perturbed strict-feedback structures with *unknown dynamics*. The proposed approach is recursive, in which the system dynamics are first decomposed into two parts, referred to as the upper and lower dynamics. The control design task is then divided into two stages, that is, designing a virtual controller for the upper dynamics, followed by synthesizing the actual controller for the full-order system. To this end, we start by collecting *noisy data* from the system through a finite-time experiment, referred to as a single trajectory. We then formulate a *data-dependent* condition as a semidefinite program, whose feasibility enables the design of a virtual controller that ensures global asymptotic stability of the origin for the upper dynamics. Building upon this virtual controller, we subsequently propose a *data-driven* sliding variable that facilitates the design of an ASSOSM controller for the unknown full-order system. This controller guarantees semi-global asymptotic stability of the origin in the presence of disturbances. Specifically, for any prescribed bounded set—no matter how large—the controller's design parameters can be chosen to ensure asymptotic stability of the origin. The effectiveness of the proposed method is demonstrated through three case studies, reflecting different aspects of the approach.

Key words: Adaptive second-order sliding mode control; data-driven control; noise-corrupted data; formal methods

1 Introduction

Controlling nonlinear systems in uncertain environments has long been a central challenge in the control community, inspiring the development of diverse strategies to manage uncertainties. Among these, sliding mode (SM) control has gained significant attention for its robustness against various uncertainties. Specifically, SM controllers drive the system's state trajectories to a predefined surface, known as the *sliding manifold*, in finite time while ensuring that they remain confined to it thereafter. Notably, system behavior on the sliding manifold remains unaffected by *matched* uncertainties (*i.e.,* uncertainties that appear only in the control input channel). Consequently, SM control design involves two main steps: *(i)* constructing an appropriate sliding variable (and the corresponding sliding manifold) to achieve the desired dynamic performance, and *(ii)* designing a control law, discontinuous on the sliding manifold, that ensures the state trajectories reach the manifold in finite time and remain on it thereafter (Ferrara et al., 2019).

Despite their advantages, SM controllers are prone to *chattering* in practical implementations, *i.e.*, high-frequency oscillations in the controlled variable caused by the finite switching rate of the control law, whereas ideal implementations assume switching at infinite frequency (Boiko et al., 2007; Levant, 2010; Utkin, 2015). Hence, higher-order sliding mode (HOSM) controllers have been introduced to mitigate chattering by shifting the essential discontinuity, needed for finite-time convergence to the sliding manifold, to a higher-order derivative of the control variable, ensuring a *continuous* control input to the system (Edwards and Sht-

⋆ This paper was not presented at any IFAC conference. Corresponding author Behrad Samari. Gian Paolo Incremona is supported by the Italian Ministry for Research in the framework of the PRIN 2022 PRIDE, grant no. 2022LP77J4.

Email addresses: b.samari2@newcastle.ac.uk (Behrad Samari), gianpaolo.incremona@polimi.it (Gian Paolo Incremona), antonella.ferrara@unipv.it (Antonella Ferrara), abolfazl.lavaei@newcastle.ac.uk (Abolfazl Lavaei).

essel, 2016; Levant, 2003). Among HOSM controllers, *second-order* sliding mode (SOSM) controllers are particularly preferred for their reduced complexity, making them more practical for implementation (Bartolini et al., 1998; Ding et al., 2018; Incremona et al., 2016). However, all these studies assume the availability of knowledge of the system model to facilitate the sliding variable design—an assumption that is often unrealistic in practical applications.

To overcome this critical challenge, two distinct yet valuable approaches have emerged: indirect and direct data-driven methods. The *indirect* approach employs system identification to construct a model, which is then used for design purposes in a model-based control manner. Yet, accurately identifying complex nonlinear systems can be computationally demanding or even infeasible (Hou and Wang, 2013; Kerschen et al., 2006). Conversely, *direct* data-driven methods, including our approach, bypass the identification phase by directly using the data gathered for design objectives. This eliminates the two-step process inherent to indirect methods, offering a more streamlined solution (Dörfler et al., 2022).

Owing to the advantages of direct data-driven approaches, a growing body of work has built upon the seminal contribution of De Persis and Tesi (2019) on stabilizing linear dynamical systems, extending the methodology to nonlinear settings. These include, but are not limited to, the stabilization of polynomial systems using noise-corrupted state-derivative data (Guo et al., 2021) and (approximate) cancellation of nonlinearities (De Persis et al., 2023). Furthermore, Taylor et al. (2021) introduce an approach for synthesizing robust controllers for nonlinear systems affected by model uncertainties, while Kenanian et al. (2019) explore data-driven stability analysis for switched systems. Moreover, Zhou et al. (2022) present a framework that achieves stabilization of unknown nonlinear systems through the simultaneous learning of a neural Lyapunov function and a nonlinear controller. Further efforts involve leveraging Petersen's lemma to design stabilizing closed-loop controllers under disturbance-corrupted input-state data (Bisoffi et al., 2022). Direct data-driven approaches have also been employed to enforce properties beyond classical stability, such as enforcing contractivity, input-to-state stability, stability of interconnected networks, and safety (Hu et al., 2025; Lavaei and Angeli, 2023; Samari and Lavaei, 2025; Samari et al., 2025b; Zaker et al., 2025a,b); see the survey by Martin et al. (2023) for recent results on direct data-driven methods. These studies, however, either do not address robustness to disturbances or assume the availability of a known disturbance bound, which appears explicitly in the proposed conditions—for instance, see Assumption 2 and Theorem 2 in the work by Hu et al. (2025).

Recently, a few data-driven SM control frameworks have been proposed to enhance robustness against disturbances and uncertainties. In this regard, Lan et al. (2024) offer an SM control design for *partially* unknown nonlinear systems, while Riva et al. (2024) and Samari et al. (2025a) present *integral* SM controllers for linear systems and interconnected networks consisting of unknown nonlinear subsystems, respectively. While promising, these approaches remain vulnerable to the chattering phenomenon, which hinders their practical deployment. In addition, Samari et al. (2025a) collect samples under disturbance-free conditions and require a predefined library of functions capable of capturing the true system dynamics—neither of which is required in our setting.

Central Contribution. Motivated by these critical challenges, we propose a direct data-driven method for designing adaptive suboptimal second-order sliding mode (ASSOSM) controllers for *fully unknown* single-input nonlinear systems within a subclass of perturbed strict-feedback dynamics. By decomposing the system into lower and upper dynamics and collecting noisy data from a finite-time experiment, we formulate a *data-dependent* condition as a semidefinite program (SDP), whose feasibility yields a virtual controller that guarantees global asymptotic stability (GAS) of the origin for the upper dynamics. Leveraging this result, we construct a *data-driven* sliding variable that enables the synthesis of an ASSOSM controller for the full-order system, ensuring semi-global asymptotic stability (S-GAS) of the origin in the presence of disturbances; that is, for any desired bounded set, the controller parameters can be tuned to render the origin asymptotically stable.

Our data-driven framework offers several practical advantages over the existing state-of-the-art approaches:

- *(i)* Unlike conventional SOSM approaches, *e.g.,* the work by Bartolini et al. (1998), that rely on system knowledge to construct the sliding variable, the proposed data-driven approach eliminates the need for a model, thereby enhancing practical applicability.
- *(ii)* By virtue of generating SOSMs, the proposed data-driven ASSOSM controller enables the mitigation of the chattering problem, which is again beneficial for practical applications.
- *(iii)* Unlike previous data-driven studies that require persistently exciting input signals in the classical sense during data collection (cf. (6)), our framework removes this assumption and additionally operates with less data (cf. Remark 2). In fact, our framework can be employed when the input signal for data collection is generated based on a feedback law (cf. Section 4.2) or even when it is constantly zero, provided that condition (5) is satisfied. This significantly enhances practicality, as generating persistently exciting inputs for nonlinear systems remains a largely unresolved challenge.
- *(iv)* The proposed unified framework simultaneously

accounts for *three distinct sources* of data noise: *(a)* noisy state derivative measurements, *(b)* unknown disturbance data, without requiring a known bound—unlike previous studies where such bounds are assumed and involved in the analysis, for instance, see (Hu et al., 2025, Assumption 2)—and *(c) noisy input data*, for which neither the noise bound nor its distribution is required. This differs from previous studies where such information explicitly appears in the analysis, *e.g.,* see (Guo et al., 2021, Remark 8).

(v) Unlike prior data-driven approaches that rely on a library of functions capable of representing the true system dynamics (Bisoffi et al., 2022; De Persis et al., 2023; Guo et al., 2021; Hu et al., 2025; Lan et al., 2024; Samari et al., 2025a), our method, for the considered class of systems, avoids this assumption, thereby reducing the required system knowledge. Furthermore, whereas Lan et al. (2024) assume that the control matrix is known, our approach does not impose this requirement.

Organization. The rest of the paper is organized as follows. In Section 2, we present the mathematical preliminaries, notation, and formal definition of the system of interest, along with an overview of the proposed approach. This is followed by a formal statement of the main problem addressed in this work. In Section 3, we first describe the data collection procedure, then present our data-driven method for constructing the sliding variable, followed by the design of the ASSOSM controller. Section 4 presents simulation results across three distinct case studies, while Section 5 concludes the paper.

2 Problem Formulation

2.1 Notation

The set of real numbers is denoted by $\mathbb{R}$, while the sets of non-negative and positive real numbers are represented by $\mathbb{R}_{\geq 0}$ and $\mathbb{R}_{>0}$, respectively. Likewise, the set of non-negative integers is expressed as $\mathbb{N}$, and the set of positive integers is denoted by $\mathbb{N}_{\geq 1}$. The identity matrix of dimension $n \times n$ is denoted by $\mathbb{I}_n$, while the zero vector of dimension n and the zero matrix of dimension $n \times m$ are denoted by $\mathbf{0}_n$ and $\mathbf{0}_{n\times m}$, respectively. The horizontal concatenation of vectors $x_i \in \mathbb{R}^n$ into an $n \times N$ matrix is expressed as $x = [x_1 \ \dots \ x_N]$. A *symmetric* matrix P is denoted as positive definite by $P \succ 0$, and as positive semi-definite by $P \succeq 0$. The transpose of a matrix P is denoted by $P^\top$. The rank of a matrix A is denoted by $\text{rank}(A)$. The Euclidean norm of a vector $x \in \mathbb{R}^n$ is represented as $\|x\|$, while $|y|$ presents the absolute value of $y \in \mathbb{R}$. In a symmetric matrix, a star $(\star)$ represents the transposed element in the symmetric position.

2.2 System Description

We start by introducing the dynamical system considered in this work, which represents a subclass of the system studied by Zhang et al. (2000).

Definition 1 (ct-PNCS) *A continuous-time perturbed nonlinear control system (CT-PNCS) evolves according to*

$$\Sigma\colon \begin{cases} \dot{x}_r = \mathcal{A}x_r + \mathbf{a}x_n, \\ \dot{x}_n = f(x) + bu + d(t), \end{cases} \tag{1}$$

where $x = [x_r^\top \ x_n]^\top \in \mathbb{R}^n$, *with* $x_r = [x_1 \ x_2 \ \dots \ x_{n-1}]^\top \in \mathbb{R}^{n-1}$, $u \in \mathbb{R}$, *and* $d : \mathbb{R}_{\geq 0} \to \mathbb{R}$ *denote, respectively, the state vector, control input, and matched disturbance. Additionally, the matrix* $\mathcal{A} \in \mathbb{R}^{(n-1)\times(n-1)}$, *the vector* $\mathbf{a} \in \mathbb{R}^{n-1}$ *with* $\mathbf{a} \neq \mathbf{0}_{n-1}$, *and the scalar* $b \in \mathbb{R}_{>0}$ *are unknown. The smooth, potentially highly nonlinear mapping* $f : \mathbb{R}^n \to \mathbb{R}$, *with* $f(\mathbf{0}_n) = 0$, *is also unknown while satisfying the following classical conditions for the existence and uniqueness of solutions:*

$$|f(x)| \leq \beta_1 + \beta_2\|x\|, \tag{2a}$$

$$\left\|\frac{\partial f(x)}{\partial x}\right\| \leq \beta_3 + \beta_4\|x\|, \tag{2b}$$

where β_1, β_2, β_3, *and* β_4 *are unknown positive constants. We use the tuple* $\Sigma = (\mathcal{A}, \mathbf{a}, f, b, d)$ *to represent the CT-PNCS in* (1), *whose components are all unknown.* □

Remark 1 (On (2a) and (2b)) *Conditions* (2a) *and* (2b) *essentially imply that:* (i) *the function* f *is globally Lipschitz-like, ensuring the existence and uniqueness of solutions for any initial condition and precluding finite escape time; and* (ii) *the magnitude of the unforced dynamics grows at most linearly with* $\|x\|$, *allowing a controller with finite amplitude to effectively regulate the system's behavior. We also note that these conditions are consistent with those commonly adopted in the model-based literature (Bartolini et al., 1998). However, we consider the positive constants* $\beta_1, \beta_2, \beta_3$, *and* β_4 *to be* unknown *in our data-driven setting, which constitutes a milder assumption.* □

As stated in Definition 1, the function f is assumed to be unknown, which is often the case in practical scenarios. To address such situations, previous data-driven studies assume that a library of functions is available for representing f (De Persis et al., 2023; Hu et al., 2025; Samari and Lavaei, 2025; Samari et al., 2025a). However, such an assumption can be restrictive in scenarios where such a library is either unavailable or not rich enough (*i.e.,* some nonlinearities are neglected) to accurately represent f. In contrast, our proposed approach in this work does not rely on this assumption, thereby reducing the

knowledge required from the system. For the sake of fairness, however, it should be acknowledged that the previously cited studies are capable of handling more general classes of nonlinear systems. Nevertheless, many classical dynamical systems, including inverted pendulums, take the form of the CT-PNCS introduced in (1) (Khalil, 2002).

We now present the assumption on the matched disturbance, as commonly adopted in sliding mode control theory (Ferrara et al., 2019).

Assumption 1 (Bounds on $d(t)$) *The matched disturbance $d(t)$ satisfies the bounds $|d(t)| < \bar{d}_1$ and $|\dot{d}(t)| < \bar{d}_2$ for all $t \in \mathbb{R}_{\geq 0}$, where $\bar{d}_1, \bar{d}_2 \in \mathbb{R}_{>0}$ are* unknown *constants.* □

With the full description of CT-PNCS Σ and the associated assumptions in place, the following subsection outlines our approach to the problem.

2.3 Design Approach

Since the ultimate objective is to design an ASSOSM controller for the CT-PNCS (1) without model knowledge, ensuring that the origin is S-GAS in the presence of the disturbance $d(t)$, we propose a two-step control design methodology that is purely based on data. More precisely, we first treat x_n as a virtual control input for the x_r-dynamics [1] of (1) and design it as a feedback law that stabilizes the upper dynamics via a Lyapunov-based argument. Based on this virtual controller, we then construct the sliding variable and design the ASSOSM control input u, which achieves semi-global stabilization in the presence of the disturbance $d(t)$.

Concretely, we define the smooth sliding variable $\sigma : \mathbb{R}^n \to \mathbb{R}$ as

$$\sigma = x_n - \varphi(x_r), \tag{3}$$

where $\varphi : \mathbb{R}^{n-1} \to \mathbb{R}$ is a smooth function satisfying $\varphi(\mathbf{0}_{n-1}) = 0$. We interpret $\varphi(x_r)$ as a virtual control input for the x_r-dynamics of (1). Since the model is unknown, φ should be designed from data to render the origin of the x_r-dynamics GAS. At the same time, the ASSOSM controller drives both σ and $\dot{\sigma}$ to zero in finite time, and as per (3), this enforces $x_n = \varphi(x_r)$. In other words, for any initial condition within an arbitrarily large prespecified bounded set, the control amplitude of the ASSOSM controller can be selected to enforce (3) to zero, *i.e.,* $\sigma = 0$, (cf. Remark 8), and thereby render the origin asymptotically stable. Specifically, since the origin is a GAS equilibrium for the x_r-dynamics under $\varphi(x_r)$ (cf. Theorem 1), it follows that, given an arbitrarily large yet bounded set, one has

$$x_r \to \mathbf{0}_{n-1} \xrightarrow{\varphi(\mathbf{0}_{n-1})=0} \varphi(x_r) \to 0 \xrightarrow[x_n=\varphi(x_r)]{\sigma=0} x_n \to 0,$$

thereby ensuring robustness with respect to the disturbance $d(t)$. As can be observed, this is a recursive design procedure, akin to the *backstepping* approach, whose outcome is the designed control input u, which ultimately attains semi-global stabilization for the full-order system in the presence of the disturbance.

It is important to note that the reason our proposed controller does not achieve global stabilization, despite the origin of the upper dynamics being GAS, is that the ASSOSM framework requires the existence of a bound (specifically, the bounds in (22), which we treat as unknown) that depends on the state variables. Clearly, if the state variables are unbounded, such a bound does not exist, and therefore the ASSOSM framework cannot be applied.

It is worth highlighting that the key motivation for employing ASSOSM control instead of its classical, *non-adaptive* counterpart (Bartolini et al., 1998) is its suitability for data-driven settings, where all required bounds are assumed to be *unknown* (cf. Definition 1, Assumption 1, and ultimately the bounds in (22)). More precisely, since the system model is unknown and only accessible through collected data, assuming the availability of these bounds would be unrealistic, rendering the approach by Bartolini et al. (1998) inapplicable; see Section 3.2 for further details. Moreover, in the unknown setting considered here, $\varphi(x_r)$ and, consequently, the sliding variable in (3) should be designed based on the collected data. With these critical challenges in mind, we now formally state the main problem addressed in this work.

Problem 1 *Consider the unknown CT-PNCS $\Sigma = (\mathcal{A}, \mathbf{a}, f, b, d)$, as in (1). By collecting a single set of noisy data from the system during a finite-time experiment, design a continuous control input that simultaneously enforces the sliding variable (3) to zero and rejects the disturbance $d(t)$, rendering the origin an S-GAS equilibrium point for the CT-PNCS (1).*

In the following section, we present our data-driven framework in detail to address Problem 1.

3 Data-Driven Framework

In this section, we introduce our data-driven ASSOSM control design. In particular, in Section 3.1, we begin by collecting noisy data from the system and show how it can be used to design $\varphi(x_r)$ such that the origin becomes a GAS equilibrium for the x_r-dynamics of the

[1] Throughout the paper, we interchangeably use the terms "x_r-dynamics" and "upper dynamics" to indicate the first dynamics given in (1).

CT-PNCS (1). Then, in Section 3.2, we present the AS-SOSM approach for designing the controller u, which drives both σ and $\dot{\sigma}$ to zero in finite time, thereby ensuring that the origin is an S-GAS equilibrium for the full-order system.

3.1 Data-Driven Sliding Variable Design

To design $\varphi(x_r)$ in a data-driven manner, we collect $\mathcal{T} \in \mathbb{N}_{\geq 1}$ samples over the time interval $[t_0, t_0+(\mathcal{T}-1)\tau]$ from the system (1), where $\tau \in \mathbb{R}_{>0}$ denotes the sampling time, yielding the following data matrices:

$$\boldsymbol{\mathcal{I}} \coloneqq \big[u(t_0)\ u(t_0+\tau)\ \dots\ u(t_0+(\mathcal{T}-1)\tau)\big], \tag{4a}$$
$$\boldsymbol{\mathcal{O}}_1 \coloneqq \big[x_r(t_0)\ x_r(t_0+\tau)\ \dots\ x_r(t_0+(\mathcal{T}-1)\tau)\big], \tag{4b}$$
$$\boldsymbol{\mathcal{O}}_2 \coloneqq \big[x_n(t_0)\ x_n(t_0+\tau)\ \dots\ x_n(t_0+(\mathcal{T}-1)\tau)\big], \tag{4c}$$
$$\dot{\boldsymbol{\mathcal{O}}}_1^+ \coloneqq \big[\dot{x}_r(t_0)\ \dot{x}_r(t_0+\tau)\ \dots\ \dot{x}_r(t_0+(\mathcal{T}-1)\tau)\big], \tag{4d}$$
$$\dot{\boldsymbol{\mathcal{O}}}_2^+ \coloneqq \big[\dot{x}_n(t_0)\ \dot{x}_n(t_0+\tau)\ \dots\ \dot{x}_n(t_0+(\mathcal{T}-1)\tau)\big], \tag{4e}$$
$$\boldsymbol{\mathcal{D}} \coloneqq \big[d(t_0)\ d(t_0+\tau)\ \dots\ d(t_0+(\mathcal{T}-1)\tau)\big], \tag{4f}$$

where data $\boldsymbol{\mathcal{D}}$ is completely unknown. In fact, compared to the relevant literature, we make no assumptions on $\boldsymbol{\mathcal{D}}$ and do not incorporate it into our analysis—a key contribution that enhances feasibility, especially when the *unknown* $\bar{d}_1$ is large; see (De Persis et al., 2023, Example 6). The reason for such a relaxation is that, instead of designing u directly, we design $\varphi(x_r)$, treating x_n as a virtual control input for the x_r-dynamics of the CT-PNCS (1). While the data $\boldsymbol{\mathcal{D}}$ affects the values of x_n, the full state x is measured during data collection, giving us access to the perturbed virtual input values x_n (cf. (4c)). This enables analysis of the input-state behavior of x_r-dynamics without explicitly considering the disturbance effect (cf. (12), where neither $\boldsymbol{\mathcal{D}}$ nor $\boldsymbol{\mathcal{I}}$ appears), making the approach inherently robust. Consequently, for the same reason, our analysis does not directly require (4a), (4e), and (4f), as they do not appear in the SDP (8) in Theorem 1, allowing us to accommodate *noisy* control input measurements without imposing any additional assumptions on the noise, including its distribution. Nevertheless, we assume that the collected samples in (4b) and (4c) follow the subsequent assumption.

Assumption 2 (Data Richness) *Assume that the matrix* $\begin{bmatrix}\boldsymbol{\mathcal{O}}_1\\ \boldsymbol{\mathcal{O}}_2\end{bmatrix}$ *has full row rank, i.e., the rank condition*

$$\operatorname{rank}\left(\begin{bmatrix}\boldsymbol{\mathcal{O}}_1\\ \boldsymbol{\mathcal{O}}_2\end{bmatrix}\right) = n \tag{5}$$

holds. □

Remark 2 (On Assumption 2) *Most previous data-driven studies are explicitly based on the so-called Willems et al.'s fundamental lemma or its generalizations (Willems et al., 2005); see (Shakouri et al., 2025) for recent insights into this lemma. For clarity of exposition, we first consider the case where the function f is linear. For the CT-PNCS (1), previous studies, e.g., (De Persis and Tesi, 2019), require*

$$\operatorname{rank}\left(\begin{bmatrix}\boldsymbol{\mathcal{O}}_1\\ \boldsymbol{\mathcal{O}}_2\\ \boldsymbol{\mathcal{I}}\end{bmatrix}\right) = n+1, \tag{6}$$

which is evidently stronger than (5). Specifically, most previous works require the input signal to be persistently exciting in order for (6) to hold.[2] *In contrast, our framework does not necessarily impose this requirement, as it is only* implicitly *based on the fundamental lemma. In particular, we interpret $\boldsymbol{\mathcal{O}}_2$ as the input signal and require only the satisfaction of (5). This distinction is significantly advantageous, as it allows us to use a feedback controller during data collection—a feature that is particularly helpful for preventing unstable behavior during experimentation (cf. Section 4.2). In contrast, previous methods cannot employ such feedback controllers during data collection, as doing so would violate (6) due to the dependency that arises between the samples $\boldsymbol{\mathcal{O}}_1, \boldsymbol{\mathcal{O}}_2$, and $\boldsymbol{\mathcal{I}}$.*

Another advantage of our condition (5) is that it requires less amount of data. Concretely, for the CT-PNCS (1), satisfying (6) requires at least $\mathcal{T} = 2n+1$ samples (De Persis and Tesi, 2019, Sec. III), whereas our condition (5) requires $\mathcal{T} = 2n-1$. Extending this reasoning to the case where $f(x)$ is nonlinear, we note that most prior studies assume the availability of a function library capable of representing $f(x)$. In such cases, condition (6) becomes remarkably stronger, and the minimum number of required samples increases significantly, depending on the size of the available library of functions (De Persis et al., 2023). In contrast, in our framework, both the required rank condition (5) and the minimum sample size $\mathcal{T} = 2n-1$ remain unchanged, even in the nonlinear case with an arbitrary function $f(x)$. We dedicate our second case study, in Section 4.2, to substantiating these arguments. □

Given that derivatives of the state at sampling times in (4d) are not directly available as measurements, we approximate them as

$$\dot{x}_i(t_0+k\tau) = \frac{x_i(t_0+(k+1)\tau) - x_i(t_0+k\tau)}{\tau} + \psi_i(t_0+k\tau),$$

with $i \in \{1,\dots,n-1\}$, and $k \in \{0,1,\dots,\mathcal{T}-1\}$,

[2] Note that the problem of designing a persistently exciting input $\boldsymbol{\mathcal{I}}$ is largely open for *nonlinear* systems—with a few exceptions, *e.g.*, the work by Alsalti et al. (2023) for some specific classes of nonlinear systems.

where the approximation error $\psi_i(t_0 + k\tau)$ is proportional to τ and can be considered as noise. Thus, we assume that (4d) is corrupted by noise

$$\Psi \coloneqq \begin{bmatrix} \psi(t_0) & \psi(t_0+\tau) & \dots & \psi(t_0+(\mathcal{T}-1)\tau) \end{bmatrix} \in \mathbb{R}^{(n-1)\times\mathcal{T}},$$

meaning that the measured data is $\boldsymbol{\mathcal{O}}_1^+ \coloneqq \hat{\boldsymbol{\mathcal{O}}}_1^+ + \Psi$. While the noise Ψ is entirely unknown, we impose the following assumption on it.

Assumption 3 (Bound on Ψ) *The unknown data matrix Ψ satisfies*

$$\Psi\Psi^\top \preceq \gamma\gamma^\top,$$

for some known $\gamma \in \mathbb{R}^{(n-1)\times\mathcal{T}}$, meaning that over the finite data collection interval, the energy of the noise remains bounded (Van Waarde et al., 2020). □

Remark 3 (On Assumption 3) *In practice, a concrete scenario where Assumption 3 holds is when a constant $\bar{\psi}$ is known such that $\|\psi(t)\|^2 \leq \bar{\psi}$ for all $t \in \mathbb{R}_{\geq 0}$, where $\psi(\cdot)$ denotes a column of Ψ. In such a case, by taking an arbitrary $y \in \mathbb{R}^{n-1}$, and by recalling the Cauchy–Schwarz inequality (Bhatia and Davis, 1995), we have*

$$\begin{aligned} y^\top\Psi\Psi^\top y &= \sum_{k=1}^{\mathcal{T}} \left(\psi_k^\top y\right)^2 \leq \sum_{k=1}^{\mathcal{T}} \|\psi_k\|^2 \|y\|^2 \\ &\leq \sum_{k=1}^{\mathcal{T}} \bar{\psi}\|y\|^2 = \bar{\psi}\mathcal{T}\|y\|^2 = y^\top\left[\bar{\psi}\mathcal{T}\mathbb{I}_{n-1}\right]y. \end{aligned}$$

Since the inequality holds for every vector y, one has

$$\Psi\Psi^\top \preceq \bar{\psi}\mathcal{T}\mathbb{I}_{n-1},$$

which implies that Assumption 3 is satisfied with $\gamma \coloneqq \sqrt{\bar{\psi}\mathcal{T}}\mathbb{I}_{n-1}$, resulting in $\gamma\gamma^\top = \bar{\psi}\mathcal{T}\mathbb{I}_{n-1}$. □

We now propose the following lemma, under which a closed-loop representation for the x_r-dynamics of the CT-PNCS (1) is obtained.

Lemma 1 (Closed-Loop Representation) *Consider the x_r-dynamics of the CT-PNCS (1). By defining $\boldsymbol{\mathcal{S}} \coloneqq [\mathbf{a} \quad \mathcal{A}]$ and designing the virtual control input as $\varphi(x_r) = \boldsymbol{\mathcal{K}}\boldsymbol{\mathcal{P}}x_r$, where $\boldsymbol{\mathcal{K}} \in \mathbb{R}^{1\times(n-1)}$ and $\boldsymbol{\mathcal{P}} \in \mathbb{R}^{(n-1)\times(n-1)}$, with $\boldsymbol{\mathcal{P}} \succ 0$, one has*

$$\dot{x}_r = \boldsymbol{\mathcal{S}}\begin{bmatrix} \boldsymbol{\mathcal{K}}\boldsymbol{\mathcal{P}} \\ \mathbb{I}_{n-1} \end{bmatrix} x_r \tag{7}$$

as the closed-loop representation. □

Proof: Considering $\boldsymbol{\mathcal{S}} = [\mathbf{a} \quad \mathcal{A}]$, and under the virtual control input $\varphi(x_r) = \boldsymbol{\mathcal{K}}\boldsymbol{\mathcal{P}}x_r$, one has

$$\begin{aligned} \dot{x}_r &= \mathcal{A}x_r + \mathbf{a}x_n = \mathcal{A}x_r + \mathbf{a}\varphi(x_r) \\ &= (\mathcal{A} + \mathbf{a}\boldsymbol{\mathcal{K}}\boldsymbol{\mathcal{P}})x_r = \boldsymbol{\mathcal{S}}\begin{bmatrix} \boldsymbol{\mathcal{K}}\boldsymbol{\mathcal{P}} \\ \mathbb{I}_{n-1} \end{bmatrix} x_r, \end{aligned}$$

concluding the proof. ■

We now offer the following theorem, as one of the main results of the work, which enables the design of a virtual control input $\varphi(x_r)$ that ensures GAS of the origin for the x_r-dynamics. Consequently, this facilitates the data-driven design of the sliding variable (3) using perturbed data collected from a finite-time experiment.

Theorem 1 (Data-Driven Design of $\varphi(x_r)$) *Given the x_r-dynamics of the CT-PNCS (1), let Assumptions 2 and 3 hold. If there exist the decision variables $\kappa_1 \in \mathbb{R}_{>0}$, $\kappa_2 \in \mathbb{R}_{\geq 0}$, $\boldsymbol{\mathcal{Q}} \in \mathbb{R}^{(n-1)\times(n-1)}$, with $\boldsymbol{\mathcal{Q}} \succ 0$, and $\boldsymbol{\mathcal{K}} \in \mathbb{R}^{1\times(n-1)}$ such that the subsequent SDP is satisfied:*

$$\begin{bmatrix} \kappa_1\mathbb{I}_{n-1} - \kappa_2(\boldsymbol{\mathcal{O}}_1^+\boldsymbol{\mathcal{O}}_1^{+\top} - \gamma\gamma^\top) & \begin{bmatrix} \boldsymbol{\mathcal{K}} \\ \boldsymbol{\mathcal{Q}} \end{bmatrix}^\top + \kappa_2\boldsymbol{\mathcal{O}}_1^+\boldsymbol{\mathcal{G}}^\top \\ \star & -\kappa_2\boldsymbol{\mathcal{G}}\boldsymbol{\mathcal{G}}^\top \end{bmatrix} \preceq 0, \tag{8}$$

where $\boldsymbol{\mathcal{G}} \coloneqq \begin{bmatrix} \boldsymbol{\mathcal{O}}_2^\top & \boldsymbol{\mathcal{O}}_1^\top \end{bmatrix}^\top$, then the state-feedback control law $\varphi(x_r) = \boldsymbol{\mathcal{K}}\boldsymbol{\mathcal{P}}x_r$, with $\boldsymbol{\mathcal{P}} \coloneqq \boldsymbol{\mathcal{Q}}^{-1} \succ 0$, renders the origin a GAS equilibrium point for the x_r-dynamics of the CT-PNCS, with a radially unbounded, continuously differentiable Lyapunov function $\mathbb{V}(x_r) = x_r^\top\boldsymbol{\mathcal{P}}x_r$. □

Proof: Consider the Lyapunov function $\mathbb{V}(x_r) = x_r^\top\boldsymbol{\mathcal{P}}x_r$ with $\boldsymbol{\mathcal{P}} \coloneqq \boldsymbol{\mathcal{Q}}^{-1}$, and hence, $\boldsymbol{\mathcal{P}}^{-1} = \boldsymbol{\mathcal{Q}}$. Under the control law $\varphi(x_r) = \boldsymbol{\mathcal{K}}\boldsymbol{\mathcal{P}}x_r$, and according to the closed-loop representation (7), we have

$$\begin{aligned} \dot{\mathbb{V}}(x_r) &= 2x_r^\top\boldsymbol{\mathcal{P}}\boldsymbol{\mathcal{S}}\begin{bmatrix} \boldsymbol{\mathcal{K}}\boldsymbol{\mathcal{P}} \\ \mathbb{I}_{n-1} \end{bmatrix} x_r \\ &= x_r^\top\left(\boldsymbol{\mathcal{P}}\boldsymbol{\mathcal{S}}\begin{bmatrix} \boldsymbol{\mathcal{K}}\boldsymbol{\mathcal{P}} \\ \mathbb{I}_{n-1} \end{bmatrix} + \begin{bmatrix} \boldsymbol{\mathcal{K}}\boldsymbol{\mathcal{P}} \\ \mathbb{I}_{n-1} \end{bmatrix}^\top \boldsymbol{\mathcal{S}}^\top\boldsymbol{\mathcal{P}}\right)x_r \\ &= x_r^\top\boldsymbol{\mathcal{P}}\left(\boldsymbol{\mathcal{S}}\begin{bmatrix} \boldsymbol{\mathcal{K}} \\ \boldsymbol{\mathcal{P}}^{-1} \end{bmatrix} + \begin{bmatrix} \boldsymbol{\mathcal{K}} \\ \boldsymbol{\mathcal{P}}^{-1} \end{bmatrix}^\top \boldsymbol{\mathcal{S}}^\top\right)\boldsymbol{\mathcal{P}}x_r. \end{aligned}$$

Accordingly, we get

$$\begin{aligned}&\dot{\mathbb{V}}(x_r)\\&= x_r^\top \boldsymbol{\mathcal{P}}\Big(\begin{bmatrix}\mathbb{I}_{n-1}\\ \boldsymbol{\mathcal{S}}^\top\end{bmatrix}^\top \begin{bmatrix}\mathbf{0}_{(n-1)\times(n-1)} & \begin{bmatrix}\boldsymbol{\mathcal{K}}\\ \boldsymbol{\mathcal{P}}^{-1}\end{bmatrix}^\top\\ \begin{bmatrix}\boldsymbol{\mathcal{K}}\\ \boldsymbol{\mathcal{P}}^{-1}\end{bmatrix} & \mathbf{0}_{n\times n}\end{bmatrix}\\&\qquad\times\begin{bmatrix}\mathbb{I}_{n-1}\\ \boldsymbol{\mathcal{S}}^\top\end{bmatrix}\Big)\boldsymbol{\mathcal{P}}x_r. \end{aligned}\tag{9}$$

The goal is to show that $\dot{\mathbb{V}}(x_r) < 0$ for all non-zero x_r. However, this is a strict inequality, which makes the implementation challenging. Thus, instead of directly enforcing $\dot{\mathbb{V}}(x_r) < 0$ for all $x_r \neq \mathbf{0}_{n-1}$, we ensure that $\dot{\mathbb{V}}(x_r) \leq -\kappa_1\, x_r^\top \boldsymbol{\mathcal{P}}\boldsymbol{\mathcal{P}} x_r$, which considering (9), is equivalent to showing

$$\underbrace{x_r^\top \boldsymbol{\mathcal{P}}\Big(\begin{bmatrix}\mathbb{I}_{n-1}\\ \boldsymbol{\mathcal{S}}^\top\end{bmatrix}^\top \overbrace{\begin{bmatrix}\kappa_1\mathbb{I}_{n-1} & \begin{bmatrix}\boldsymbol{\mathcal{K}}\\ \boldsymbol{\mathcal{P}}^{-1}\end{bmatrix}^\top\\ \begin{bmatrix}\boldsymbol{\mathcal{K}}\\ \boldsymbol{\mathcal{P}}^{-1}\end{bmatrix} & \mathbf{0}_{n\times n}\end{bmatrix}}^{\Xi_1}\begin{bmatrix}\mathbb{I}_{n-1}\\ \boldsymbol{\mathcal{S}}^\top\end{bmatrix}\Big)\boldsymbol{\mathcal{P}}x_r}_{\mathcal{F}} \leq 0.\tag{10}$$

If (10) is enforced, since $\kappa_1 \in \mathbb{R}_{>0}$ and $\boldsymbol{\mathcal{P}} \succ 0$, it becomes evident that $\dot{\mathbb{V}}(x_r) < 0$ for all $x_r \neq \mathbf{0}_{n-1}$, rendering the origin of the x_r-dynamics GAS under the control law $\varphi(x_r) = \boldsymbol{\mathcal{K}}\boldsymbol{\mathcal{P}}x_r$.

Concurrently, Assumption 3 can also be reformulated as

$$\begin{bmatrix}\mathbb{I}_{n-1}\\ \Psi^\top\end{bmatrix}^\top \begin{bmatrix}-\gamma\gamma^\top & \mathbf{0}_{(n-1)\times\mathcal{T}}\\ \star & \mathbb{I}_{\mathcal{T}}\end{bmatrix}\begin{bmatrix}\mathbb{I}_{n-1}\\ \Psi^\top\end{bmatrix} \preceq 0.\tag{11}$$

Furthermore, and according to the x_r-dynamics of the CT-PNCS (1), we know that the data gathered satisfies

$$\boldsymbol{\mathcal{O}}_1^+ = \mathcal{A}\boldsymbol{\mathcal{O}}_1 + \mathbf{a}\boldsymbol{\mathcal{O}}_2 + \Psi.\tag{12}$$

Then, considering $\boldsymbol{\mathcal{S}} = [\mathbf{a}\ \mathcal{A}]$ and $\boldsymbol{\mathcal{G}} = \begin{bmatrix}\boldsymbol{\mathcal{O}}_2^\top & \boldsymbol{\mathcal{O}}_1^\top\end{bmatrix}^\top$, we have

$$\boldsymbol{\mathcal{O}}_1^+ \overset{(12)}{=} \boldsymbol{\mathcal{S}}\boldsymbol{\mathcal{G}} + \Psi \Rightarrow \Psi = \boldsymbol{\mathcal{O}}_1^+ - \boldsymbol{\mathcal{S}}\boldsymbol{\mathcal{G}}.$$

Hence, (11) can be rewritten as

$$-\gamma\gamma^\top + (\boldsymbol{\mathcal{O}}_1^+ - \boldsymbol{\mathcal{S}}\boldsymbol{\mathcal{G}})(\boldsymbol{\mathcal{O}}_1^+ - \boldsymbol{\mathcal{S}}\boldsymbol{\mathcal{G}})^\top \preceq 0,$$

or equivalently

$$\begin{bmatrix}\mathbb{I}_{n-1}\\ \boldsymbol{\mathcal{S}}^\top\end{bmatrix}^\top \overbrace{\begin{bmatrix}\boldsymbol{\mathcal{O}}_1^+\boldsymbol{\mathcal{O}}_1^{+\top} - \gamma\gamma^\top & -\boldsymbol{\mathcal{O}}_1^+\boldsymbol{\mathcal{G}}^\top\\ \star & \boldsymbol{\mathcal{G}}\boldsymbol{\mathcal{G}}^\top\end{bmatrix}}^{\Xi_2}\begin{bmatrix}\mathbb{I}_{n-1}\\ \boldsymbol{\mathcal{S}}^\top\end{bmatrix} \preceq 0.\tag{13}$$

Considering (13), and by defining

$$\mathcal{E} := x_r^\top \boldsymbol{\mathcal{P}}\begin{bmatrix}\mathbb{I}_{n-1}\\ \boldsymbol{\mathcal{S}}^\top\end{bmatrix}^\top \begin{bmatrix}\boldsymbol{\mathcal{O}}_1^+\boldsymbol{\mathcal{O}}_1^{+\top} - \gamma\gamma^\top & -\boldsymbol{\mathcal{O}}_1^+\boldsymbol{\mathcal{G}}^\top\\ \star & \boldsymbol{\mathcal{G}}\boldsymbol{\mathcal{G}}^\top\end{bmatrix}\begin{bmatrix}\mathbb{I}_{n-1}\\ \boldsymbol{\mathcal{S}}^\top\end{bmatrix}\boldsymbol{\mathcal{P}}x_r,$$

we simply get $\mathcal{E} \leq 0$. Now, utilizing the classical S-procedure (Yakubovich et al., 2004), we can show that $\dot{\mathbb{V}}(x_r) \leq -\kappa_1\, x_r^\top \boldsymbol{\mathcal{P}}\boldsymbol{\mathcal{P}} x_r < 0$ for all non-zero x_r, while respecting $\mathcal{E} \leq 0$. More concretely, by defining $z := \begin{bmatrix}\mathbb{I}_{n-1}\\ \boldsymbol{\mathcal{S}}^\top\end{bmatrix}\boldsymbol{\mathcal{P}}x_r$, we have $\mathcal{F} = z^\top \Xi_1 z$ and $\mathcal{E} = z^\top \Xi_2 z \leq 0$. Then, according to the S-procedure, if there exists a non-negative multiplier $\kappa_2 \in \mathbb{R}_{\geq 0}$ such that

$$\Xi_1 - \kappa_2\, \Xi_2 \preceq 0,\tag{14}$$

or equivalently

$$\begin{bmatrix}\kappa_1\mathbb{I}_{n-1} - \kappa_2(\boldsymbol{\mathcal{O}}_1^+\boldsymbol{\mathcal{O}}_1^{+\top} - \gamma\gamma^\top) & \begin{bmatrix}\boldsymbol{\mathcal{K}}\\ \boldsymbol{\mathcal{Q}}\end{bmatrix}^\top + \kappa_2\boldsymbol{\mathcal{O}}_1^+\boldsymbol{\mathcal{G}}^\top\\ \star & -\kappa_2\boldsymbol{\mathcal{G}}\boldsymbol{\mathcal{G}}^\top\end{bmatrix} \preceq 0,$$

which is exactly our proposed condition in (8), we can conclude

$$z^\top \Xi_2 z \leq 0 \implies \underbrace{z^\top \Xi_1 z}_{\dot{V}(x_r)+\kappa_1\, x_r^\top \boldsymbol{\mathcal{P}}\boldsymbol{\mathcal{P}}x_r} \leq 0,\tag{15}$$

ensuring that

$$\dot{V}(x_r) \leq -\kappa_1\, x_r^\top \boldsymbol{\mathcal{P}}\boldsymbol{\mathcal{P}} x_r < 0,$$

for all $x_r \neq \mathbf{0}_{n-1}$. This renders the origin a GAS equilibrium for the x_r-dynamics under the control law $\varphi(x_r) = \boldsymbol{\mathcal{K}}\boldsymbol{\mathcal{P}}x_r$, thereby concluding the proof. ■

We emphasize that the matrix $\boldsymbol{\mathcal{S}} := [\mathbf{a}\quad \mathcal{A}]$ is entirely unknown in the closed-loop representation (7). Importantly, we neither identify $\boldsymbol{\mathcal{S}}$ at any stage nor require it in our proposed SDP (8). This fact alone substantiates that the upper dynamics are not identified. Instead, leveraging the closed-loop representation, we propose the SDP (8) to design the virtual controller directly from noisy data, without relying on knowledge of $\mathcal{A}$, $\mathbf{a}$, or their compact form $\boldsymbol{\mathcal{S}}$.

Remark 4 (On Condition (5)) *Due to fulfilling condition (5) in Assumption 2 when gathering data, it is guaranteed that* $\boldsymbol{\mathcal{G}}\boldsymbol{\mathcal{G}}^\top \succ 0$*, which is required for the feasibility of the SDP (8). This highlights the necessity of imposing Assumption 2, with its various aspects discussed in Remark 2.* □

Remark 5 (On Scalability) *The dimensions of the decision variables in the SDP (8) depend only on the number of state variables in the* x_r*-dynamics, i.e.,* $n-1$ *rather than* n*. This implies that even when the function* f *in (1) is linear, the proposed SDP scales more efficiently to high-dimensional systems compared to previous data-driven approaches, and this advantage becomes even more pronounced when* f *is nonlinear. In fact, in the nonlinear case, as mentioned earlier, previous studies require access to an extensive library of functions to represent the function* f*, with the dimensions of the decision variables depending on the size of that library. These considerations highlight the superior scalability of our framework. We also note that the SDP (8) is linear in all decision variables, with no bilinear terms; it can be efficiently solved using standard SDP solvers, such as* YALMIP *(Lofberg, 2004) in combination with* MOSEK *(ApS, 2019).* □

Remark 6 (Role of Noisy Data) *We note that the data* $\boldsymbol{\mathcal{O}}_2$*, derived from the* x_n*–dynamics, is significantly influenced by both the noisy input data* $\boldsymbol{\mathcal{I}}$ *and the disturbance* $\boldsymbol{\mathcal{D}}$*; it enters the SDP (8) through* $\boldsymbol{\mathcal{G}}$*. The derivative data* $\boldsymbol{\mathcal{O}}_1^+$ *is likewise noise-corrupted and appears in the SDP (8). Although* $\boldsymbol{\mathcal{I}}$ *is not explicit in (8), its influence is fully captured via* $\boldsymbol{\mathcal{O}}_2$*. In fact, the reason that* $\boldsymbol{\mathcal{I}}$ *does not explicitly appear in the SDP (8) is that* x_n *is treated as the virtual control input for the* x_r*-dynamics. Consequently, the influence of* $\boldsymbol{\mathcal{I}}$ *does not manifest itself directly in the* x_r*-dynamics. This claim is supported by (12), where* $\boldsymbol{\mathcal{I}}$ *does not appear. This absence is precisely what enables our approach to handle noisy input data without requiring any additional assumptions.* □

Having offered the SDP (8) to design the virtual control input $\varphi(x_r)$, we now proceed with presenting our data-driven ASSOSM control framework in the following subsection.

3.2 ASSOSM Controller Design

Here, we describe the design of the ASSOSM controller based on the data-driven results established in Section 3.1. We show that the sliding variable σ depends on the data-driven components $\boldsymbol{\mathcal{K}}$ and $\boldsymbol{\mathcal{P}}$, which are obtained according to Theorem 1, and consequently, the ASSOSM controller also depends on them.

We first recall that according to (3) and Theorem 1, the proposed data-driven sliding variable is

$$\sigma = x_n - \boldsymbol{\mathcal{K}}\boldsymbol{\mathcal{P}}x_r. \tag{16}$$

We now proceed to design the ASSOSM controller to ensure that the sliding variable (16) and its time derivative converge to zero in finite time. Before that, however, it is worthwhile to highlight several important aspects of the approach. First, we note that standard SM and SOSM control approaches (Bartolini et al., 1998) require knowledge of certain bounds (cf. the bounds in (22)), which is not feasible in our setting due to the unavailability of the system model. By employing the ASSOSM control framework, we circumvent this classical requirement, making the approach more suitable for a data-driven context. Second, by utilizing the ASSOSM framework, the matched disturbance is actively rejected, rendering the origin S-GAS even in the presence of a non-vanishing disturbance $d(t)$, thereby enabling a robustified data-driven design. This contrasts with previous data-driven approaches, which typically yield feedback control laws that do not guarantee asymptotic stability of the origin under non-vanishing disturbances. Finally, the resulting control input is *continuous*, which offers a clear advantage in practical implementations.

To proceed with the design, we note that interpreting (16) as the output of the CT-PNCS (1), the resulting input–output map has relative degree one.[3] However, designing the ASSOSM controller, which yields a continuous control input, requires artificially increasing the relative degree to two. To do so, we introduce the auxiliary variables $\varsigma_1 := \sigma$ and $\varsigma_2 := \dot{\sigma}$, while constructing the auxiliary system

$$\dot{\varsigma}_1 = \varsigma_2, \qquad \dot{\varsigma}_2 = \Delta + \Lambda\nu, \tag{17}$$

where

$$\Delta = \frac{\partial f(x)}{\partial x}\begin{bmatrix} \mathcal{A}x_r + \mathbf{a}x_n \\ f(x) + bu + d(t) \end{bmatrix} + \dot{d}(t) - \boldsymbol{\mathcal{K}}\boldsymbol{\mathcal{P}}\mathcal{A}(\mathcal{A}x_r + \mathbf{a}x_n) - \boldsymbol{\mathcal{K}}\boldsymbol{\mathcal{P}}\mathbf{a}(f(x) + bu + d(t)), \tag{18a}$$

$$\Lambda = b, \tag{18b}$$

are both unknown. Moreover, $\dot{u} = \nu$, where $\nu \in \mathbb{R}$ denotes the discontinuous control input that is to be designed to ensure that ς_1 and ς_2 reach zero in finite time, even in the presence of the disturbance $d(t)$.

It is evident that ς_2 is unmeasurable, as it depends on the disturbance $d(t)$, which is unknown. However, to design ν such that it drives both ς_1 and ς_2 to zero in finite time, and in particular to design the adaptation law, the value of ς_2 at each time instant is required. To this end, we

[3] That is, the control input u appears explicitly in the first derivative of the sliding variable (16), *i.e.,* $\dot{\sigma}$.

employ Levant's differentiator (Levant, 1998, 2003) to estimate ς_2 with high accuracy—in theory, the estimate becomes exact after a finite time. More concretely, to estimate ς_2 using Levant's differentiator, we have

$$\dot{\hat{\varsigma}}_1 = -\mu_0 \left|\hat{\varsigma} - \varsigma_1\right|^{\frac{1}{2}} \operatorname{sign}(\hat{\varsigma} - \varsigma_1) + \hat{\varsigma}_2, \tag{19a}$$

$$\dot{\hat{\varsigma}}_2 = -\mu_1 \operatorname{sign}(\hat{\varsigma} - \varsigma_1), \tag{19b}$$

where $\hat{\varsigma}_1$ and $\hat{\varsigma}_2$ denote the estimates of ς_1 and ς_2, respectively. Additionally, $\mu_0 = 1.5\,\mathcal{L}^{\frac{1}{2}}$ and $\mu_1 = 1.1\,\mathcal{L}$, where $\mathcal{L} \in \mathbb{R}_{>0}$ is the design parameter of the differentiator. It is important to allow Levant's differentiator (19) sufficient time to converge in order to obtain a reliable estimate of ς_2. Notably, the differentiator is proven to converge in finite time. In particular, increasing the design parameter $\mathcal{L}$ accelerates convergence. However, excessively large values of $\mathcal{L}$ can introduce fluctuations in the estimates of ς_2, potentially causing practical implementation issues. Thus, selecting $\mathcal{L}$ should involve a trade-off between convergence speed and estimation robustness.

Having adopted Levant's differentiator to estimate ς_2, we can now design the following discontinuous control input ν to drive both ς_1 and ς_2 to zero in finite time (Incremona et al., 2016):

$$\nu = -\Upsilon_{\text{ad}} \operatorname{sign}\Big(\varsigma_1 - \frac{1}{2}\varsigma_1^{\max}\Big), \tag{20a}$$

where Υ_{ad} is the adaptive control amplitude to be designed, and $\varsigma_1^{\max}$ denotes the extremal value of ς_1 along its trajectory. To design Υ_{ad}, we have

$$\dot{\Upsilon}_{\text{ad}} = \begin{cases} \eta_1|\varsigma_1| + \eta_2|\hat{\varsigma}_2|, & \text{if } |\varsigma_1| > |\Theta|, \\ 0, & \text{otherwise,} \end{cases} \tag{20b}$$

where $\eta_1, \eta_2 \in \mathbb{R}_{>0}$ are design parameters, Θ denotes the maximum value of the sequence ς_1, stored as $\varsigma_1^{\max}$, and $\Upsilon_{\text{ad}}(t_0) = \Upsilon_{\text{ad}_0}$. We note that while the input ν is discontinuous, the actual control input $u = \int_{t_0}^{t} \nu(s)\mathrm{d}s$ remains continuous.

Remark 7 (On Computing $\varsigma_1^{\max}$) *In addition to estimating ς_2, Levant's differentiator (19) can also be employed to compute $\varsigma_1^{\max}$ by storing the value of ς_1 at time instants when the sign of $\hat{\varsigma}_2$ changes. The corresponding procedure is illustrated in Fig. 1.* □

It is crucial to note that in the non-adaptive version (Bartolini et al., 1998), the control amplitude Υ_{ad} is constant and must satisfy

$$\Upsilon_{\text{ad}} = \Upsilon_{\text{ad}_0} > \max\Big\{\frac{\bar{\Delta}}{\underline{\Lambda}}, \frac{4\bar{\Delta}}{3\underline{\Lambda} - \bar{\Lambda}}\Big\}, \tag{21}$$

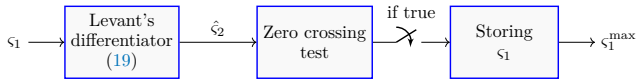

Fig. 1. Schematic illustration of using Levant's differentiator (19) to compute $\varsigma_1^{\max}$.

where $\bar{\Delta}$, $\underline{\Lambda}$, and $\bar{\Lambda}$ are *known* positive constants satisfying

$$|\Delta| \leq \bar{\Delta}, \quad \underline{\Lambda} \leq \Lambda \leq \bar{\Lambda}. \tag{22}$$

However, it is evident that finding such bounds on (18a) and (18b) is nearly impossible, particularly in our data-driven setting, where all components of the system are unknown (cf. Definition 1 and Assumption 1), thus demonstrating the advantage of adopting the ASSOSM control framework.

Remark 8 (On (20b)) *We note that in (20b), the control amplitude Υ_{ad} increases adaptively when the magnitude of the sliding variable tends to exceed that of Θ; otherwise, Υ_{ad} retains its previous value. As shown by Incremona et al. (2016), if Υ_{ad} is updated according to (20b), it satisfies (21) in finite time. Consequently, as demonstrated by Bartolini et al. (1998), ς_1 and ς_2 reach zero in finite time, thereby steering the sliding variable (16) and its time derivative to zero. Recalling (2) and noting that the bounds in (22) exist over any bounded domain—regardless of its size—we conclude that there exists a finite Υ_{ad} that satisfies (21). It is worth noting that larger values of η_1 and η_2 enable Υ_{ad} to satisfy (21) more rapidly, but this comes at the cost of increased control effort u. Therefore, a trade-off should be considered when choosing these parameters.* □

The following theorem, as another main result of this work, establishes that the origin is an S-GAS equilibrium for the system under the control input u, given that both σ and $\dot{\sigma}$ converge to zero in finite time.

Theorem 2 (Convergence to $\sigma = 0$) *Let Assumptions 1-3 hold. Consider the auxiliary system (17) under the discontinuous control input ν defined in (20a), with the adaptive control amplitude Υ_{ad} given by (20b), along with Levant's differentiator (19). Assume that $t_0 \geq t_{\mathcal{L}}$, with $t_{\mathcal{L}}$ being the finite time required for the convergence of the differentiator. Then, within a finite time $t_r \geq t_d \geq t_0$, where t_d is the time instant at which (21) holds, the auxiliary system state variables ς_1 and ς_2 are driven to the origin of the auxiliary system's state space. That is, a sliding mode $\sigma = 0$, with σ defined in (16), is enforced, i.e.,*

$$x_n = \boldsymbol{\mathcal{K}}\boldsymbol{\mathcal{P}} x_r, \tag{23}$$

thereby rendering the origin an S-GAS equilibrium for the CT-PNCS (1) under the continuous control input $\dot{u} = \nu$. □

Proof: Since we employ Levant's differentiator and assume $t_0 \geq t_{\mathcal{L}}$, the value of ς_2 is known exactly, as the estimate $\hat{\varsigma}_2$ becomes theoretically exact after a finite time, as previously discussed. This implies that the extremal value $\varsigma_1^{\max}$ can, in principle, be detected with ideal accuracy using the procedure outlined in Remark 7. Simultaneously, according to Remark 8, the control amplitude Υ_{ad} increases adaptively until it satisfies (21) in finite time t_d. Hence, one gets $\exists t_r \geq t_d \geq t_0$: $\sigma(t) = \dot{\sigma}(t) = 0,\ \forall t \geq t_r$, where t_r is called the *reaching time*. Once the sliding variable (16) is enforced to zero, (23) follows directly. Moreover, since the bounds in (22) exist within any arbitrarily large yet bounded domain, a finite Υ_{ad} satisfying (21) also exists. Therefore, there always exists a discontinuous control input ν that drives ς_1 and ς_2 to the origin of the auxiliary system's state space.

In addition, the x_r-dynamics of the CT-PNCS (1) possess a GAS equilibrium at the origin under $\varphi(x_r) = \boldsymbol{\mathcal{K}}\boldsymbol{\mathcal{P}}x_r$ (cf. Theorem 1), ensuring that no initial condition leads to divergence of either x_r or $\varphi(x_r)$. Thus, since there always exists a discontinuous control input ν that drives ς_1 and ς_2 to the origin of the auxiliary system's state space, one can also conclude that the continuous control input $\dot{u} = \nu$ achieves semi-global stabilization despite the existence of the disturbance $d(t)$, rendering the origin an S-GAS equilibrium point for the closed-loop system, thereby concluding the proof. ■

We present Algorithm 1, which outlines all the necessary steps for designing the proposed data-driven ASSOSM controller.

Algorithm 1 Data-driven design of ASSOSM control

Require: Assumptions 1–3, $\bar{\psi}$
1: Collect $\boldsymbol{\mathcal{O}}_1$, $\boldsymbol{\mathcal{O}}_2$, and $\boldsymbol{\mathcal{O}}_1^+$ as in (4)
2: Compute noise bound $\gamma\gamma^\top$ according to Remark 3 based on $\bar{\psi}$
3: Obtain $\boldsymbol{\mathcal{K}}$, $\boldsymbol{\mathcal{Q}}$, κ_1, and κ_2 by solving the SDP (8)
4: Compute $\boldsymbol{\mathcal{P}}$ as $\boldsymbol{\mathcal{Q}}^{-1}$
5: Design the virtual control input $\varphi(x_r) = \boldsymbol{\mathcal{K}}\boldsymbol{\mathcal{P}}x_r$ as in Theorem 1
6: Construct the sliding variable σ as in (3)
7: Employ Levant's differentiator (19) to estimate ς_2
8: Design the adaptive Υ_{ad} as in (20b)
9: Compute $\varsigma_1^{\max}$ according to Fig. 1
10: Design the discontinuous input ν as in (20a)
11: Compute the continuous control input $u = \int_{t_0}^{t} \nu(s)\mathrm{d}s$
Ensure: Semi-global stabilizer u, disturbance rejection

4 Simulation Results

In this section, we demonstrate the effectiveness of the proposed data-driven framework through three case studies. Specifically, the first case study highlights the practicality of our framework on real-world systems; the second illustrates the discussion in Remark 2 regarding the full-row-rank assumption on data; and the third demonstrates the applicability of our approach to systems with a highly nonlinear function f, as well as its ability to achieve semi-global stabilization for systems whose states are initialized with arbitrarily large values. All simulations were conducted using MATLAB *R2023b* on a MacBook Pro with an Apple M2 Max chip and 32 GB of memory.

4.1 Physical Benchmark: Inverted Pendulum

The first benchmark illustrates the practical applicability of the proposed data-driven framework on a physical system. To this end, we consider the inverted pendulum described by Khalil (2002, Example 13.21), whose dynamics are given by

$$\Sigma : \begin{cases} \dot{x}_1 = x_2, \\ \dot{x}_2 = -10\sin(x_1) - x_2 + 10u + d(t). \end{cases} \tag{24}$$

We note that (24) conforms to the structure of the CT-PNCS (1) with $\mathcal{A} = 0$, $\mathbf{a} = 1$, $b = 10$, and $f(x) = -10\sin(x_1) - x_2$, all of which are assumed to be fully unknown. The considered disturbance is also given in Fig. 2c. The goal is to design an ASSOSM controller for the unknown system (24) using a noisy data trajectory, thereby demonstrating the practicality of our proposed framework.

To this end, we first collect noisy data by applying the arbitrary input $u = 0.1\cos(t)$ and setting the initial condition to $x(0) = [1 \quad 1]^\top$. We note that this choice of controller is used solely for data collection. The sampling time is set to $\tau = 0.1$, and we gather $\mathcal{T} = 3$ samples, which is the minimum required according to Remark 2. It is worth recalling that in (De Persis et al., 2023, Example 1), for a disturbance-free discrete-time inverted pendulum system, 10 noise-free samples were required, which underscores the data efficiency of our framework. We assume that the noise Ψ follows a uniform distribution over the interval $[-0.5, 0.5]$. Thus, according to Remark 3, we have $\gamma\gamma^\top = 0.75$. Then, we collect the following data to proceed with the further steps:

$$\begin{bmatrix} \boldsymbol{\mathcal{O}}_1 \\ \boldsymbol{\mathcal{O}}_2 \\ \boldsymbol{\mathcal{O}}_1^+ \end{bmatrix} = \begin{bmatrix} 1 & 1.0588 & 1.0397 \\ 1 & 0.1857 & -0.5515 \\ 0.9366 & -0.5117 & -1.3232 \end{bmatrix}.$$

Utilizing this data and solving the SDP in (8), we obtain

$$\boldsymbol{\mathcal{K}} = -0.7343, \quad \boldsymbol{\mathcal{Q}} = 0.6708 \Rightarrow \boldsymbol{\mathcal{P}} = 1.4907,$$
$$\kappa_1 = 0.5134, \quad \kappa_2 = 0.4990.$$

Thus, according to Theorem 1, the virtual control input is given by $\varphi(x_r) = -1.0946\,x_1$, resulting in the sliding variable (16) being obtained as $\sigma = x_2 + 1.0946\,x_1$.

Following the procedure described in Section 3.2, we now design the ASSOSM controller. The design parameter of Levant's differentiator (19) is selected as $\mathcal{L} = 300$. For the adaptive control amplitude Υ_{ad}, defined in (20b), we set $\Upsilon_{\text{ad}_0} = 1$, $\eta_1 = 30$, and $\eta_2 = 15$. Moreover, $\varsigma_1^{\max}$ is determined according to the procedure illustrated in Fig. 1. The discontinuous control input ν is obtained as in (20a), and accordingly, the continuous control input u is computed. In Fig. 2, the simulation results for the unknown system (24) under the designed ASSOSM controller u are presented. As observed, the results are in complete agreement with the theoretical predictions.

It is worthwhile mentioning that if a sufficiently rich function library for $f(x)$ is not available—*i.e.*, the system nonlinearity is neglected, as discussed by De Persis et al. (2023, Example 7) for the discrete-time case—three key shortcomings arise, which also apply to the continuous-time setting. First, one should assume that the neglected nonlinearity is bounded with a known bound, which can be restrictive in practical scenarios. Second, the experiment for data collection should be performed from an initial condition very close to the equilibrium. Finally, although the result guarantees that the origin is asymptotically stable, an estimate of the region of attraction should still be obtained for the completeness of the analysis.

On the other hand, since our framework does not require a library of functions for f, all of these difficulties are avoided. Moreover, as the proposed controller achieves semi-global stabilization, the region of attraction can be arbitrarily enlarged to include any given compact set—regardless of its size—by appropriately adjusting the controller parameters (cf. the third benchmark in Section 4.3).

4.2 Comparison Benchmark

The purpose of the second benchmark is to substantiate the arguments presented in Remark 2 and to draw a comparison with the work by De Persis and Tesi (2019). For the sake of clarity, we consider a simple linear system, whose dynamics evolve according to

$$\Sigma : \begin{cases} \dot{x}_1 = x_2, \\ \dot{x}_2 = x_1 + x_2 + u + d(t). \end{cases} \tag{25}$$

The system model is assumed to be completely unknown. Moreover, for now, we assume the system is not subject to any disturbance (*i.e.*, $d(t) \equiv 0$), with noise-free state-derivative data. As is evident, the open-loop system is unstable, which makes data collection challenging even over short time periods. For instance, starting from $x(0) = [2 \quad 3]^\top$ with a sampling time of $\tau = 0.5$, the magnitudes of both state variables exceed 100 at $t = 2.5$ seconds—after collecting just 5 samples, the minimum required to apply the results of De Persis and Tesi (2019)—potentially causing severe damage to the sys-

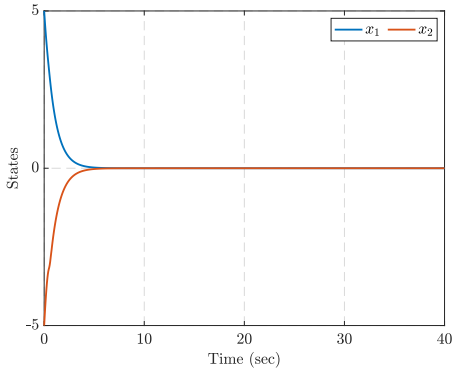

(a) State variables evolution

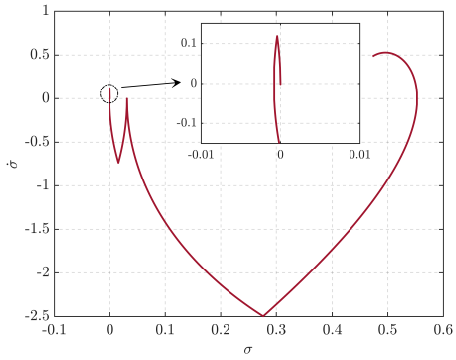

(b) Auxiliary system trajectory

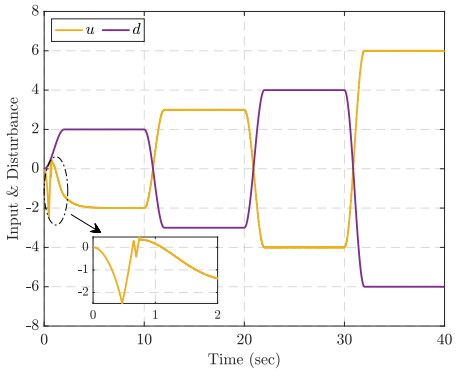

(c) Control input u and disturbance d over time

Fig. 2. **Inverted Pendulum.** Fig. 2a illustrates the evolution of the state variables over time from the initial condition $x(0) = [5 \quad -5]^\top$, showing convergence to the origin under the designed controller. Fig. 2b depicts the phase portrait of the auxiliary system (17), demonstrating that the sliding variable σ is steered to zero. Fig. 2c illustrates that the designed control input effectively rejects the disturbance and drives the system state toward the sliding manifold, thereby ensuring the asymptotic stability of the origin.

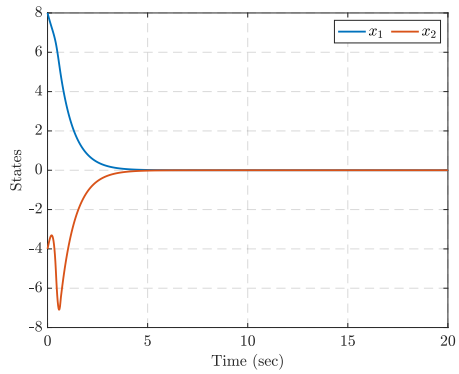

(a) State variables evolution

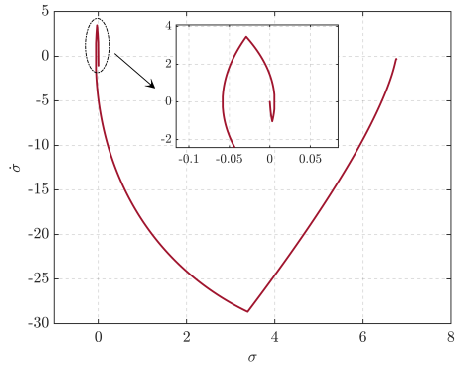

(b) Auxiliary system trajectory

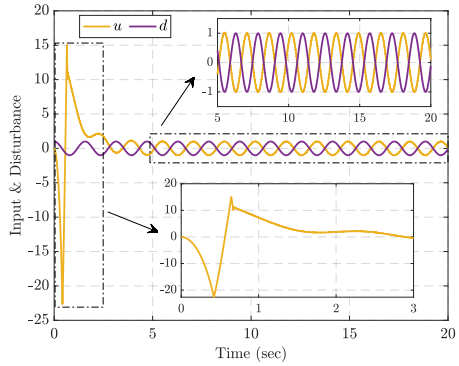

(c) Control input u and disturbance d over time

Fig. 3. **Comparison Benchmark.** Fig. 3a displays the state trajectories from the initial condition $x(0) = [8 \ -4]^\top$, confirming convergence to the origin. Fig. 3b provides the phase portrait of the auxiliary system (17), illustrating that the sliding variable σ is steered to zero. Fig. 3c demonstrates that the controller rejects the disturbance while driving the state variables to the sliding manifold.

tem.

To address the above issue, one possible solution is to employ a feedback controller during data collection. For instance, suppose that prior knowledge about system (25) indicates that, under the feedback law $u = -2x_1 - x_2$, the system exhibits oscillatory rather than unstable behavior. However, using the indicated control input for data collection violates condition (6) in Remark 2, thereby preventing the application of the results of De Persis and Tesi (2019). More concretely, in the noise-free case and following (De Persis and Tesi, 2019, Remark 2), by defining

$$X_{1,\mathcal{T}} := \begin{bmatrix} \mathcal{O}_1^+ \\ \mathcal{O}_2^+ \end{bmatrix}, \quad X_{0,\mathcal{T}} := \begin{bmatrix} \mathcal{O}_1 \\ \mathcal{O}_2 \end{bmatrix}, \quad U_{0,1,\mathcal{T}} := \mathcal{I},$$

if there exists a matrix $Q \in \mathbb{R}^{\mathcal{T} \times n}$ satisfying

$$\begin{cases} X_{1,\mathcal{T}} Q + Q^\top X_{1,\mathcal{T}}^\top \prec 0, \\ X_{0,\mathcal{T}} Q \succ 0, \end{cases} \tag{26}$$

then $u = Kx$, with $K = U_{0,1,\mathcal{T}} Q (X_{0,\mathcal{T}} Q)^{-1}$, is a stabilizing controller for (25). However, it is evident that if one collects data using $u = -2x_1 - x_2$, then

$$U_{0,1,\mathcal{T}} = \begin{bmatrix} -2 & -1 \end{bmatrix} X_{0,\mathcal{T}},$$

and, therefore, we get

$$\begin{aligned} u = Kx &= U_{0,1,\mathcal{T}} Q (X_{0,\mathcal{T}} Q)^{-1} x \\ &= \begin{bmatrix} -2 & -1 \end{bmatrix} \underbrace{\overbrace{X_{0,\mathcal{T}} Q}^{\succ 0} (X_{0,\mathcal{T}} Q)^{-1}}_{\mathcal{I}_n} x = -2x_1 - x_2, \end{aligned}$$

which corresponds to the control input used for data collection. However, it is not a stabilizing controller for system (25). This confirms that violation of condition (6) in Remark 2 precludes the use of the method in (De Persis and Tesi, 2019), even if condition (26) is satisfied.

To demonstrate the effectiveness of our approach on this benchmark, we revisit system (25), now considering $d(t) = \cos(t)$. The sampling time is set to $\tau = 0.5$, and the initial condition is chosen as $x(0) = [2 \ 3]^\top$. We collect $\mathcal{T} = 3$ samples under the same input $u = -2x_1 - x_2$. The noise Ψ is assumed to follow a uniform distribution over the interval $[-1, 1]$. Hence, according to Remark 3, we obtain $\gamma\gamma^\top = 3$. The collected samples are presented as

$$\begin{bmatrix} \mathcal{O}_1 \\ \mathcal{O}_2 \\ \mathcal{O}_1^+ \end{bmatrix} = \begin{bmatrix} 2 & 3.3133 & 4.0258 \\ 3 & 2.1330 & 0.6289 \\ 3.3242 & 0.7827 & -1.1786 \end{bmatrix}.$$

Solving the SDP (8) with this data results in

$$\begin{aligned} &\mathcal{K} = -0.3924, \quad \mathcal{Q} = 0.2915 \Rightarrow \mathcal{P} = 3.4305, \\ &\kappa_1 = 0.2278, \quad \kappa_2 = 0.0655, \quad \sigma = x_2 + 1.3461 x_1. \end{aligned}$$

Now, we proceed to design the ASSOSM controller. To do so, we consider the exact parameters mentioned in Section 4.1. Fig. 3 presents the simulation results of applying the designed ASSOSM controller to system (25), demonstrating the effectiveness of our approach.

We note that our framework is not only capable of handling scenarios in which samples are collected under a feedback controller, but it can also be employed when no input is applied during data collection, provided that the samples satisfy condition (5) in Assumption 2.

4.3 Highly-Nonlinear Benchmark

The final benchmark aims to demonstrate that our proposed framework can handle highly nonlinear dynamics, for which obtaining a representative library of functions, as required in previous works, is challenging. It also demonstrates that the proposed ASSOSM controller achieves semi-global stabilization from a significantly large initial condition. To this end, we consider the system

$$\Sigma : \begin{cases} \dot{x}_1 = -x_1 + x_2, \\ \dot{x}_2 = -x_2 + x_3, \\ \dot{x}_3 = -x_3 + x_4, \\ \dot{x}_4 = \ln(1 + \sin^2(x_1 x_2)) + \frac{x_3}{1+x_3^2} + u + d(t), \end{cases} \tag{27}$$

where the system dynamics are assumed to be fully unknown. The disturbance is $d(t) = \tanh(t)$.

Similarly to the previous benchmarks, we begin by collecting noisy data from the system. To do so, we set the initial condition to $x(0) = [7 \ -7 \ \ 3.5 \ -3.5]^\top$. The sampling time is $\tau = 0.5$, and we collect $\mathcal{T} = 15$ samples. During data collection, the input applied to the system is $u = -\sin(t)$. The noise Ψ is assumed to follow a uniform distribution over the interval $[-0.1, 0.1]$, resulting in $\gamma\gamma^\top = 0.45\mathbb{I}_3$. Due to the relatively large number of samples, the resulting data matrices are not reported for the sake of brevity. However, the parameters obtained by solving the SDP (8) are provided as follows:

$$\mathcal{K} = \begin{bmatrix} -0.2832 \\ 0.2328 \\ -0.1733 \end{bmatrix}^\top, \ \mathcal{P} = \begin{bmatrix} 20.2193 & 8.1914 & -21.1564 \\ 8.1914 & 8.9159 & -2.7685 \\ -21.1564 & -2.7685 & 31.4177 \end{bmatrix},$$

with $\kappa_1 = 0.0018$ and $\kappa_2 = 0.0142$, resulting in the sliding variable $\sigma = x_4 + 0.1539x_1 - 0.2355x_2 + 0.0961x_3$. For the ASSOSM control design, all parameters are selected as in Section 4.1, except for the design parameter of Levant's differentiator (19), which is set to $\mathcal{L} = 3 \times 10^5$. This choice is motivated by the fact that, in this benchmark, we consider large initial conditions and therefore require the estimate $\hat{\varsigma}_2$ to converge to the true value of ς_2 more rapidly.

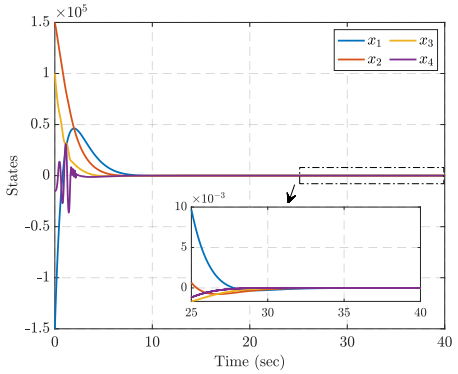

(a) State variables evolution

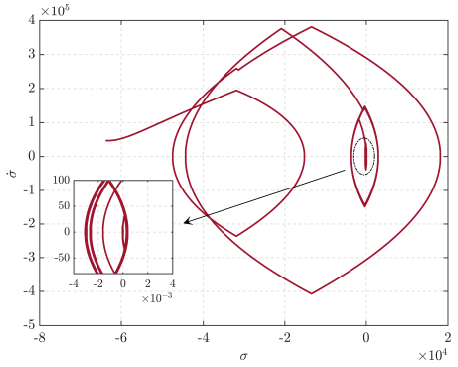

(b) Auxiliary system trajectory

Fig. 4. **Highly-Nonlinear Benchmark.** Fig. 4a shows the evolution of the state variables from significantly large initial conditions (in the order of 10^5), illustrating convergence to the origin. Fig. 4b depicts the phase portrait of the auxiliary system, demonstrating that the sliding variable σ is driven to zero.

The simulation results for this benchmark are presented in Fig. 4. As shown, despite the large initial conditions, in the order of 10^5, the designed controller successfully steers the sliding variable σ to zero, thereby rendering the origin asymptotically stable. Nonetheless, it is worth noting that the selection of design parameters plays a key role, particularly when the initial condition is selected in a large bounded domain.

5 Conclusions

In this work, we developed a direct data-driven approach for designing ASSOSM controllers for unknown single-input nonlinear systems with perturbed strict-feedback dynamics. The system was decomposed into lower and upper subsystems, and noisy data from a finite-time experiment enabled the formulation of a data-dependent condition as an SDP. Accordingly, the feasibility of the proposed SDP yielded a virtual controller that ensured

GAS of the origin for the upper dynamics. Building on this result, we constructed a data-driven sliding variable to synthesize an ASSOSM controller for the full-order system, ensuring S-GAS of the origin despite the presence of disturbances. Extending this work to more general system models and HOSM controllers is a promising future research direction.

References

M. Alsalti, V. G. Lopez, and M. A. Müller. On the design of persistently exciting inputs for data-driven control of linear and nonlinear systems. *IEEE Control Systems Letters*, 7:2629–2634, 2023.

M. ApS. Mosek optimization toolbox for MATLAB. *User's Guide and Reference Manual, Version*, 4(1): 116, 2019.

G. Bartolini, A. Ferrara, and E. Usai. Chattering avoidance by second-order sliding mode control. *IEEE Transactions on Automatic Control*, 43(2):241–246, 1998.

R. Bhatia and C. Davis. A Cauchy-Schwarz inequality for operators with applications. *Linear Algebra and its Applications*, 223:119–129, 1995.

A. Bisoffi, C. De Persis, and P. Tesi. Data-driven control via Petersen's lemma. *Automatica*, 145, 2022.

I. Boiko, L. Fridman, A. Pisano, and E. Usai. Analysis of chattering in systems with second-order sliding modes. *IEEE Transactions on Automatic Control*, 52 (11):2085–2102, 2007.

C. De Persis and P. Tesi. Formulas for data-driven control: Stabilization, optimality, and robustness. *IEEE Transactions on Automatic Control*, 65(3):909–924, 2019.

C. De Persis, M. Rotulo, and P. Tesi. Learning controllers from data via approximate nonlinearity cancellation. *IEEE Transactions on Automatic Control*, 68(10):6082–6097, 2023.

S. Ding, K. Mei, and S. Li. A new second-order sliding mode and its application to nonlinear constrained systems. *IEEE Transactions on Automatic Control*, 64(6):2545–2552, 2018.

F. Dörfler, J. Coulson, and I. Markovsky. Bridging direct and indirect data-driven control formulations via regularizations and relaxations. *IEEE Transactions on Automatic Control*, 68(2):883–897, 2022.

C. Edwards and Y. B. Shtessel. Adaptive continuous higher order sliding mode control. *Automatica*, 65: 183–190, 2016.

A. Ferrara, G. P. Incremona, and M. Cucuzzella. *Advanced and optimization based sliding mode control: Theory and applications*. SIAM, 2019.

M. Guo, C. De Persis, and P. Tesi. Data-driven stabilization of nonlinear polynomial systems with noisy data. *IEEE Transactions on Automatic Control*, 67 (8):4210–4217, 2021.

Z.-S. Hou and Z. Wang. From model-based control to data-driven control: Survey, classification and perspective. *Information Sciences*, 235:3–35, 2013.

Z. Hu, C. De Persis, and P. Tesi. Enforcing contraction via data. *IEEE Transactions on Automatic Control*, 2025.

G. P. Incremona, M. Cucuzzella, and A. Ferrara. Adaptive suboptimal second-order sliding mode control for microgrids. *International Journal of Control*, 89(9): 1849–1867, 2016.

J. Kenanian, A. Balkan, R. M. Jungers, and P. Tabuada. Data driven stability analysis of black-box switched linear systems. *Automatica*, 109, 2019.

G. Kerschen, K. Worden, A. F. Vakakis, and J.-C. Golinval. Past, present and future of nonlinear system identification in structural dynamics. *Mechanical Systems and Signal Processing*, 20(3):505–592, 2006.

H. K. Khalil. *Nonlinear systems*, volume 3. Prentice hall Upper Saddle River, NJ, 2002.

J. Lan, X. Zhao, and C. Sun. Data-driven sliding mode control for partially unknown nonlinear systems. *arXiv:2403.16136*, 2024.

A. Lavaei and D. Angeli. Data-driven stability certificate of interconnected homogeneous networks via ISS properties. *IEEE Control Systems Letters*, 7:2395–2400, 2023.

A. Levant. Robust exact differentiation via sliding mode technique. *Automatica*, 34(3):379–384, 1998.

A. Levant. Higher-order sliding modes, differentiation and output-feedback control. *International Journal of Control*, 76(9-10):924–941, 2003.

A. Levant. Chattering analysis. *IEEE Transactions on Automatic Control*, 55(6):1380–1389, 2010.

J. Lofberg. YALMIP: A toolbox for modeling and optimization in MATLAB. In *Proceedings of International Conference on Robotics and Automation*, pages 284–289. IEEE, 2004.

T. Martin, T. B. Schön, and F. Allgöwer. Guarantees for data-driven control of nonlinear systems using semidefinite programming: A survey. *Annual Reviews in Control*, 56, 2023.

G. Riva, G. P. Incremona, S. Formentin, and A. Ferrara. A data-driven approach for integral sliding mode control design. In *Proceedings of the 63rd Conference on Decision and Control (CDC)*, pages 6825–6830, 2024.

B. Samari and A. Lavaei. Data-driven dynamic controller synthesis for discrete-time general nonlinear systems. In *Proceedings of the 28th ACM International Conference on Hybrid Systems: Computation and Control (HSCC)*, pages 1–12, 2025.

B. Samari, G. P. Incremona, A. Ferrara, and A. Lavaei. From data to sliding mode control of uncertain large-scale networks with unknown dynamics. *arXiv:2502.19806*, 2025a.

B. Samari, M. Zaker, and A. Lavaei. Abstraction-based control of unknown continuous-space models with just two trajectories. In *Proceedings of the 7th Annual Learning for Dynamics & Control Conference (L4DC)*, volume 283 of *Proceedings of Machine Learning Research*, pages 1167–1179. PMLR, 2025b.

A. Shakouri, H. J. van Waarde, and M. K. Camlibel.

A new perspective on Willems' fundamental lemma: Universality of persistently exciting inputs. *IEEE Control Systems Letters*, 2025.

A. J. Taylor, V. D. Dorobantu, S. Dean, B. Recht, Y. Yue, and A. D. Ames. Towards robust data-driven control synthesis for nonlinear systems with actuation uncertainty. In *Proceedings of the 60th IEEE Conference on Decision and Control (CDC)*, pages 6469–6476, 2021.

V. Utkin. Discussion aspects of high-order sliding mode control. *IEEE Transactions on Automatic Control*, 61 (3):829–833, 2015.

H. J. Van Waarde, M. K. Camlibel, and M. Mesbahi. From noisy data to feedback controllers: Nonconservative design via a matrix S-lemma. *IEEE Transactions on Automatic Control*, 67(1):162–175, 2020.

J. C. Willems, P. Rapisarda, I. Markovsky, and B. L. De Moor. A note on persistency of excitation. *Systems & Control Letters*, 54(4):325–329, 2005.

V. A. Yakubovich, G. A. Leonov, and A. K. Gelig. *Stability of stationary sets in control systems with discontinuous nonlinearities*, volume 14. World Scientific Singapore, 2004.

M. Zaker, D. Angeli, and A. Lavaei. Certified learning of incremental ISS controllers for unknown nonlinear polynomial dynamics. In *Proceedings of the 64th IEEE Conference on Decision and Control (CDC 2025) - arXiv: 2412.03901*, 2025a.

M. Zaker, A. Nejati, and A. Lavaei. From data to global asymptotic stability of unknown large-scale networks with provable guarantees. In *Proceedings of the 28th ACM International Conference on Hybrid Systems: Computation and Control*, pages 1–14, 2025b.

T. Zhang, S. S. Ge, and C. C. Hang. Adaptive neural network control for strict-feedback nonlinear systems using backstepping design. *Automatica*, 36(12):1835–1846, 2000.

R. Zhou, T. Quartz, H. De Sterck, and J. Liu. Neural Lyapunov control of unknown nonlinear systems with stability guarantees. *Advances in Neural Information Processing Systems*, 35:29113–29125, 2022.